

Hierarchical Self-Assembly of a Biomimetic Diblock Copolypeptoid into Homochiral Superhelices

Hannah K. Murnen,[†] Adrienne M. Rosales,[†] Jonathan N. Jaworski,[§]
Rachel A. Segalman,^{*,†,‡} and Ronald N. Zuckermann^{*,‡,§}

Department of Chemical and Biomolecular Engineering, University of California,
Berkeley, California 94720, and Molecular Foundry, Materials Science Division, Lawrence
Berkeley National Laboratory, 1 Cyclotron Road, Berkeley, California 94720

Received July 16, 2010; E-mail: rnzuckermann@lbl.gov; segalman@berkeley.edu

Abstract: The aqueous self-assembly of a sequence-specific bioinspired peptoid diblock copolymer into monodisperse superhelices is demonstrated to be the result of a hierarchical process, strongly dependent on the charging level of the molecule. The partially charged amphiphilic diblock copolypeptoid 30-mer, [*N*-(2-phenethyl)glycine]₁₅-[*N*-(2-carboxyethyl)glycine]₁₅, forms superhelices in high yields, with diameters of 624 ± 69 nm and lengths ranging from 2 to 20 μm . Chemical analogs coupled with X-ray scattering and crystallography of a model compound have been used to develop a hierarchical model of self-assembly. Lamellar stacks roll up to form a supramolecular double helical structure with the internal ordering of the stacks being mediated by crystalline aromatic side chain–side chain interactions within the hydrophobic block. The role of electrostatic and hydrogen bonding interactions in the hydrophilic block is also investigated and found to be important in the self-assembly process.

Introduction

Hierarchical self-assembly is a hallmark of biological materials. Systems ranging from nacre¹ to collagen fibrils² have been heralded for their mechanical strength stemming from their unique layered structures. The precise order of these biomaterials on the micrometer and millimeter scales arises from atomically defined interactions at the nanometer and even subnanometer level. Understanding the relationship between these interactions has great implications for the design of new materials with controllable order across many length scales.³

Although examples of hierarchical polypeptide structures abound in nature,^{4–6} the *de novo* design of such systems is still a major challenge.⁷ While progress has been made in the design of simple polypeptide motifs, the molecular complexity of polypeptide interactions makes it difficult to engineer their self-assembly into complex or hierarchical structures. Hydrophobic and ionic forces are joined by backbone chirality and hydrogen bonding, making it challenging to isolate or understand the effect

of any parameter in particular. Thus, most efforts in the *de novo* design of folded and self-assembling peptides have focused on relatively short chain lengths.^{8–14} The utility of engineered peptide structures in the design of structured biomaterials has been proven by the diversity of achievable structures including flat or twisted tapes, tubes, and spheres,^{13,15} as well as by the insights gained into the mechanisms of amyloid^{16,17} and collagen^{11,12,18} fibril formation. *De novo* peptide systems are thus attractive for specific biotechnological applications,³ but simpler biomimetic polymer systems may allow the development of straightforward design rules for the engineering of self-assembled materials. Therefore, a tunable and synthetically robust system that can mimic the atomic level ordering in biological systems while allowing system engineering is desired for both materials applications and fundamental investigations of biomacromolecular self-assembly.

[†] University of California.

[‡] Materials Science Division, Lawrence Berkeley National Laboratory.
[§] Molecular Foundry, Lawrence Berkeley National Laboratory.

- (1) Fritz, M.; Morse, D. E. *Curr. Opin. Colloid Interface Sci.* **1998**, *3*, 55–62.
(2) Ottani, V.; Martini, D.; Franchi, M.; Ruggeri, A.; Raspanti, M. *Micron* **2002**, *33*, 587–596.
(3) Rajagopal, K.; Schneider, J. P. *Curr. Opin. Struct. Biol.* **2004**, *14*, 480–486.
(4) Wong, G. C. L.; Tang, J. X.; Lin, A.; Li, Y. L.; Janmey, P. A.; Safinya, C. R. *Science* **2000**, *288*, 2035–2039.
(5) Raviv, U.; Needleman, D. J.; Li, Y. L.; Miller, H. P.; Wilson, L.; Safinya, C. R. *Proc. Natl. Acad. Sci. U.S.A.* **2005**, *102*, 11167–11172.
(6) Audette, G. F.; van Schalk, E. J.; Hazes, B.; Irvin, R. T. *Nano Lett.* **2004**, *4*, 1897–1902.
(7) Schueler-Furman, O.; Wang, C.; Bradley, P.; Misura, K.; Baker, D. *Science* **2005**, *310*, 638–642.

- (8) Lamm, M. S.; Rajagopal, K.; Schneider, J. P.; Pochan, D. J. *J. Am. Chem. Soc.* **2005**, *127*, 16692–16700.
(9) Venkatraman, J.; Shankaramma, S. C.; Balaram, P. *Chem. Rev.* **2001**, *101*, 3131–3152.
(10) Saiani, A.; Mohammed, A.; Frielinghaus, H.; Collins, R.; Hodson, N.; Kielty, C. M.; Sherratt, M. J.; Miller, A. F. *Soft Matter* **2009**, *5*, 193–202.
(11) Fallas, J. A.; O’Leary, L. E. R.; Hartgerink, J. D. *Chem. Soc. Rev.* **2010**, *39*, 3510–3527.
(12) Khew, S. T.; Tong, Y. W. *Biochemistry* **2008**, *47*, 585–596.
(13) Adams, D. J.; Holtzmann, K.; Schneider, C.; Butler, M. F. *Langmuir* **2007**, *23*, 12729–12736.
(14) Nagarkar, R. P.; Hule, R. A.; Pochan, D. J.; Schneider, J. P. *J. Am. Chem. Soc.* **2008**, *130*, 4466–4474.
(15) Gazit, E. *Chem. Soc. Rev.* **2007**, *36*, 1263–1269.
(16) Marini, D. M.; Hwang, W.; Lauffenburger, D. A.; Zhang, S. G.; Kamm, R. D. *Nano Lett.* **2002**, *2*, 295–299.
(17) de la Paz, M. L.; Goldie, K.; Zurdo, J.; Lacroix, E.; Dobson, C. M.; Hoenger, A.; Serrano, L. *Proc. Natl. Acad. Sci. U.S.A.* **2002**, *99*, 16052–16057.
(18) Woolfson, D. N. *Biopolymers* **2010**, *94*, 118–127.

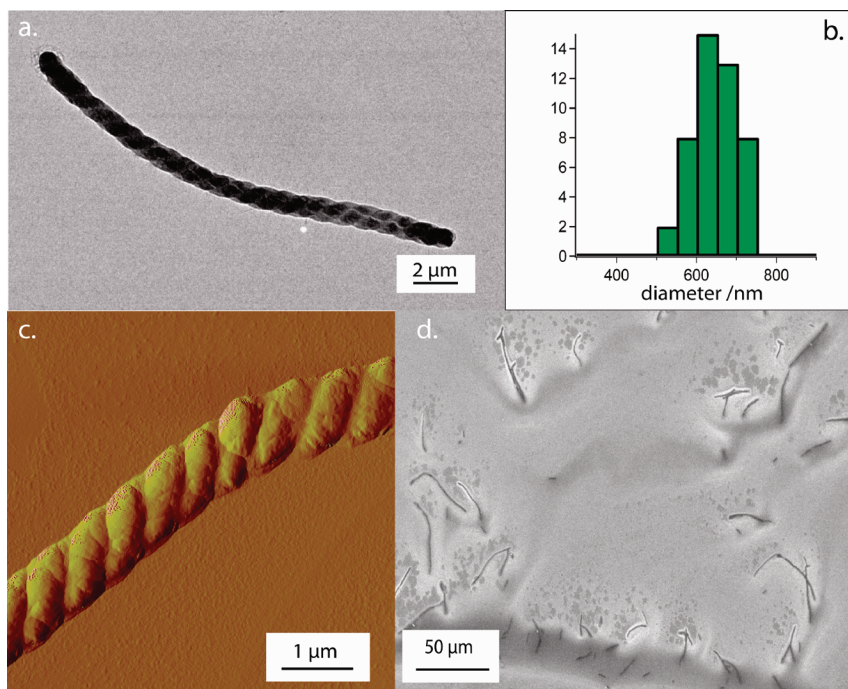


Figure 3. Helix formation from $p\text{Npe}_{15}\text{Nce}_{15}$ occurs after 3–7 days in aqueous solution at a pH of 6.8. The helices are 624 ± 69 nm in diameter (the histogram is shown in b) and range from 2 to 40 μm in length. They can be seen in TEM (a), AFM (c), or SEM in backscatter electron mode (d). A zoomed out image (c) shows the abundance of the structures within one sample.

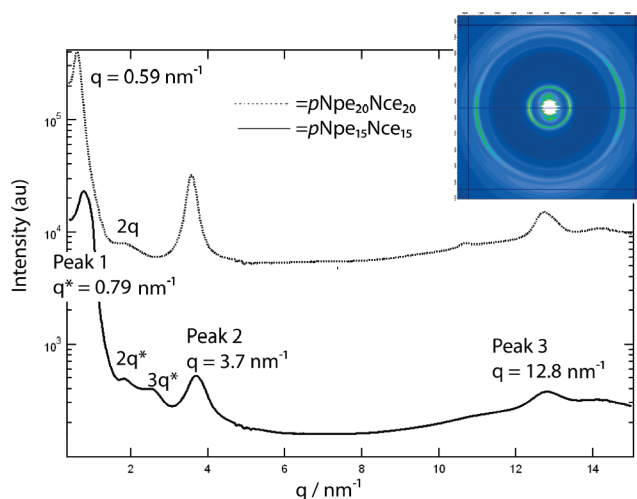


Figure 4. Synchrotron X-ray scattering was performed on an evaporated helix sample to investigate the internal ordering. The dotted line here represents $p\text{Npe}_{15}\text{Nce}_{15}$ while the solid line is $p\text{Npe}_{20}\text{Nce}_{20}$. The peaks marked q^* , $2q^*$, and $3q^*$ indicate a lamellar stacking with a d spacing of 7.8 nm, very similar to the thickness of the sheets. The peaks marked 2 and 3 are crystalline peaks at d spacings of 1.66 nm and 4.8 Å respectively and are hypothesized to be intrachain packing as modeled in Figure 1.

stacks within a double helix. In addition, there are also peaks at $q = 3.7$ and 12.8 nm^{-1} which correspond to d -spacings of 1.66 nm and 4.8 Å (labeled peaks 2 and 3 respectively in Figure 4). These peaks are attributed to crystalline packing between chains (Figure 2a). The 1.66 nm dimension corresponds to the distance between two chains packed inside the supramolecular helix (side chain crystallinity) with the 2-phenethyl groups facing each in other in what is most likely an edge-to-face orientation as seen in Figure 2a. The 4.8 Å dimension corresponds to the neighboring interbackbone distance as shown in Figure 2a.

An anisotropic 2D scattering pattern (Figure 4, inset) supports the model put forth in Figure 2. Importantly, the crystalline

peaks are perpendicular to the lamellar peaks (the arc at the lowest q) as would be expected from the model in Figure 2. Due to the presence of multiple grains and the twisting of the helix, both of the crystalline peaks are seen in the meridional direction even though in any individual sheet they are perpendicular to each other. The anisotropy appears in the scattering only after centrifugal (as opposed to static) evaporation, indicating the centrifugation causes some partial alignment of the helices. The scattering pattern is similar to that observed in amyloid fibrils^{48–50} and helices formed from amyloid β peptide fragments⁵¹ where the meridional peaks are cited as evidence of a cross- β structure.

To further confirm the assignment of the lamellar and intramolecular crystalline peaks, specific chemical modifications were made to both the main chain and the side chain lengths of the polymer. The resulting changes in the X-ray scattering peaks were used to verify the origin of the peaks. First, the overall length of the polymer was increased from 15 monomers of each block to 20 monomers of each block forming the 40mer $p\text{Npe}_{20}\text{Nce}_{20}$. This had the effect of decreasing the q -value for the primary peak, q^* , from 0.79 nm^{-1} to 0.59 nm^{-1} , demonstrating an increase in the lamellar spacing by 2.64 nm (Figure 4, dotted line). This was corroborated by AFM analysis showing the thickness of the sheets formed by $p\text{Npe}_{20}\text{Nce}_{20}$ to be 9.9 ± 0.66 nm. The scattering and AFM confirmed that the lamellar q^* , $2q^*$, and $3q^*$ peaks do stem from polymer chains extended in the lengthwise direction and also that these lamellar peaks are linked to the sheet thickness. As predicted by the model in Figure 2, the location of the crystalline peaks between side

(48) Blake, C.; Serpell, L. *Structure* **1996**, *4*, 989–998.

(49) Sunde, M.; Serpell, L. C.; Bartlam, M.; Fraser, P. E.; Pepys, M. B.; Blake, C. C. F. *J. Mol. Biol.* **1997**, *273*, 729–739.

(50) Serpell, L. C. *Biochim. Biophys. Acta: Mol. Basis Dis.* **2000**, *1502*, 16–30.

(51) Castelletto, V.; Hamley, I. W.; Hule, R. A.; Pochan, D. *Angew. Chem., Int. Ed.* **2009**, *48*, 2317–2320.

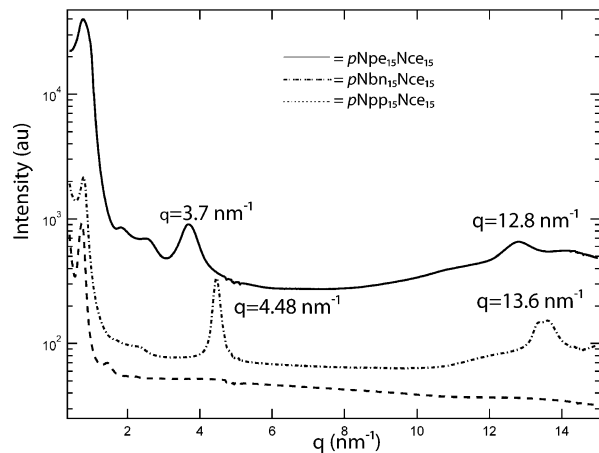


Figure 5. X-ray scattering on helical samples of $p\text{Npe}_{15}\text{Nce}_{15}$ (solid), $\text{pNbN}_{15}\text{Nce}_{15}$ (perforated), and $p\text{Npp}_{15}\text{Nce}_{15}$ (dashed). The lamellar peaks at $d = 7.8 \text{ nm}$ remain in each sample. However, in the $p\text{NbN}_{15}\text{Nce}_{15}$ sample, the crystalline peaks have shifted to higher q indicating a smaller spacing. The shift in the peak originally at 3.7 nm^{-1} has now shifted to 4.48 nm^{-1} which corresponds to two C–C bonds. The peak originally at 12.8 nm^{-1} has shifted to 13.6 nm^{-1} . It is not clear where the size of this shift originates.

chains (peaks 2 and 3 in Figure 4) was not altered by this chemical modification since they stem only from the packing of the side chains, which have not been changed in this case.

Additional chemical modifications were made to investigate the higher q peaks attributed to intrachain packing. The length of the 2-phenylethyl side chain was shortened by one methylene unit to create *N*-(benzyl)glycine-*b*-*N*-(2-carboxyethyl)glycine ($p\text{NbN}_{15}\text{Nce}_{15}$, Table 2). This molecule also forms a superhelix when self-assembled in aqueous solution. The peak which originally corresponded to a d -spacing of 1.66 nm shifts to reflect a d -spacing of 1.37 nm , resulting in a difference of 2.9 Å (Figure 5). This is reasonable given a C–C bond length of 1.54 Å and a crystalline arrangement with the phenyl groups facing each other such that a one carbon change in the side chain linkage actually results in a distance decrease of two carbon–carbon bonds (Figure 2). The peak originally corresponding to a 4.8 Å spacing shifts to a d -spacing of 4.5 Å . This peak, as shown in Figure 2a, does not depend directly on side chain length so it is likely that, with a smaller side chain, the backbones can simply pack slightly closer together. The length of the phenyl side chain was also increased by one methylene unit to form *N*-(3-phenylpropyl)glycine-*b*-*N*-(2-carboxyethyl)glycine ($p\text{Npp}_{15}\text{Nce}_{15}$, Table 2), which also formed superhelices. However, in this case the side chain crystalline peaks disappear, indicating that crystallization is not present within the helices (Figure 5). The longer side chains are more flexible and therefore more difficult to crystallize. This is corroborated by differential scanning calorimetry data (Supporting Information, Figure S5) indicating that the *N*-(3-phenylpropyl)glycine homopolymer does not crystallize in the solid state whereas the 2-phenethyl homopolymer does.²⁸ Crystallization of the hydrophobic block is therefore not an essential factor in the overall formation of the superhelices.

Simply using chemical modifications can only give indirect evidence of the atomic structure within the helix. To gain further insight into the details of the atomic order in the hydrophobic block, a model compound was synthesized and crystallized. Because symmetric cycloalkanes and *N*-methylated cyclic

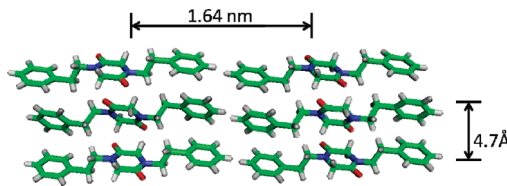


Figure 6. Crystal structure of a model cyclic dipeptoid 1,4-bis-(2-phenethyl)-piperazine-2,5-dione showing the packing geometry of the 2-phenylethyl groups. Green represents carbon atoms, blue represents nitrogen, red represents oxygen, and white represents hydrogen. The dimensions shown match those seen in X-ray scattering of a superhelix.

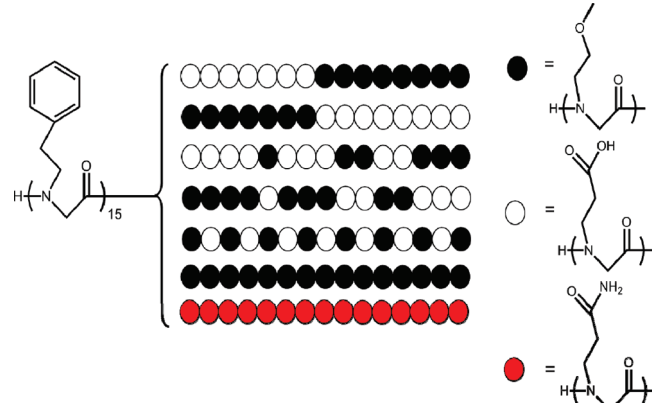


Figure 7. A set of closely related sequences was designed to pin the chargeable groups at specific locations. The hydrophobic portion of the molecule was held constant while the hydrophilic block was altered. The solid circles represent 2-methoxyethyl side chains which have a similar hydrophilicity to the carboxyethyl side chains (○) but cannot be charged. The red circles represent *N*-(2-carboxamidoethyl) side chains which have similar hydrogen bonding capabilities as the carboxyethyl side chains, but cannot be charged.

dipeptides have been shown to readily crystallize,^{52,53} we prepared a cyclic dipeptoid, 1,4-bis-(2-phenethyl)-piperazine-2,5-dione, that displays the same *N*-2-phenethyl side chain groups present in the diblock. It is hypothesized that cyclized dipeptoids could serve as a model system to gain insight into the packing of these side chains within a larger structure. The atomic structure of the cyclic *N*-2-phenethyl dipeptoid was determined by X-ray crystallography (Figure 6) as a comparison to $p\text{Npe}_{15}\text{Nce}_{15}$.

The phenethyl groups are aligned with one another in a staggered edge-to-face conformation to form a plane (Figure 6). Lamellar stacks of these planes result in aromatic faces pointing directly toward each other. The spacings observed from the X-ray scattering of the $p\text{Npe}_{15}\text{Nce}_{15}$ helices (1.66 nm and 4.8 Å , respectively, Figure 4) match the dimensions shown in the diketopiperazine crystal structure corresponding to the side chain and main chain packing distances (1.64 nm and 4.7 Å , respectively, Figure 7a). Similarly, the spacings observed from the X-ray scattering of the $p\text{NbN}_{15}\text{Nce}_{15}$ helices (1.37 nm and 4.5 Å , respectively, Figure 5) match the side chain packing and the backbone (central ring) spacing dimensions shown in the

(52) Palacin, S.; Chin, D. N.; Simanek, E. E.; MacDonald, J. C.; Whitesides, G. M.; McBride, M. T.; Palmore, G. T. *R. J. Am. Chem. Soc.* **1997**, *119*, 11807–11816.

(53) Benedetti, E.; Marsh, R. E.; Goodman, M. *J. Am. Chem. Soc.* **1976**, *98*, 6676–6684.

could account for the homochirality. However, self-assembly has occurred in both hydrophilic (glass) and hydrophobic (plastic) vials indicating that the surface probably does not play a large role in the self-assembly. As expected, circular dichroism of the superhelices has shown no optical rotation of light (Supporting Information, Figure S7) demonstrating that the chirality is not on a molecular length scale. The shape of the molecule is another potential source of asymmetry, and neutron scattering is being pursued as a future experiment to test this possibility. The last possibility is the presence of unequal surface stresses on the lamellae as they form. This has previously been shown to cause preferential bending of the lamellae in one direction or the other.^{70–72} It is not clear in this case what would cause unequal surface stresses although they cannot be ruled out as a potential chirality inducer.

Conclusion

In conclusion, a remarkable homochiral biomimetic structure has been discovered resulting from the self-assembly of an amphiphilic partially charged diblock copolypeptoid of defined sequence. The hierarchical internal ordering of the assemblies has been characterized in detail using X-ray scattering coupled with precise chemical modifications. The crystal structure of a small model molecule supports the model of self-assembly. While the origin of the homochirality of these structures remains a mystery, it is clear that the interplay of hydrophobic and

electrostatic forces is crucial to the formation of such a complex structure. The highly ordered microscale self-assembly described here demonstrates the power of polypeptoids to serve as an ideal system for engineering and understanding biomacromolecular self-assembly across several length scales.

Acknowledgment. This work was supported by the Office of Naval Research in the form of a Presidential Early Career Award in Science and Engineering (PECASE) for R.A.S. Polypeptoid synthesis and associated chemical characterization were performed at the Molecular Foundry, and XRD experiments were performed at the Advanced Light Source (ALS). Both are Lawrence Berkeley National Laboratory user facilities supported by the Office of Science, Office of Basic Energy Sciences, U.S. Department of Energy, under Contract No. DE-AC02-05CH11231. The authors thank Dr. James Holton and George Meigs for experimental assistance and Dr. Gary Ren for helpful discussions. H.K.M. acknowledges the Department of Defense for an NDSEG fellowship, and A.M.R. acknowledges the National Science Foundation for a graduate fellowship. J.N.J. acknowledges the Defense Threat Reduction Agency for financial support.

Supporting Information Available: Analytical HPLC and MALDI spectra for polypeptoids, quantification of self-assembly, base titration curve for *pNpe₁₅Nce₁₅*, comparison of X-ray scattering in the solid state and in solution, differential scanning calorimetry data, electron microscopy images, circular dichroism spectroscopy, and X-ray crystallography data for 1,4-bis-(2-phenethyl)-piperazine-2,5-dione. This material is available free of charge via the Internet at <http://pubs.acs.org>.

JA106340F

- (70) Keith, H. D.; Padden, F. J. *Polymer* **1984**, *25*, 28–42.
(71) Lotz, B.; Cheng, S. Z. D. *Polymer* **2005**, *46*, 577–610.
(72) Ye, H.-M.; Wang, J.-S.; Tang, S.; Xu, J.; Feng, X.-Q.; Guo, B.-H.; Xie, X.-M.; Zhou, J.-J.; Li, L.; Wu, Q.; Chen, G.-Q. *Macromolecules* **2010**, *43*, 5762–5770.